

# A Machine Learning Approach to Optimal Inverse Discrete Cosine Transform (IDCT) Design

Yifan Wang\*, Zhanxuan Mei\*, Chia-Yang Tsai†, Ioannis Katsavounidis† and C.-C. Jay Kuo\*

\*University of Southern California, Los Angeles, California, USA

† Facebook, Inc., Menlo Park, California, USA

**Abstract**—The design of the optimal inverse discrete cosine transform (IDCT) to compensate the quantization error is proposed for effective lossy image compression in this work. The forward and inverse DCTs are designed in pair in current image/video coding standards without taking the quantization effect into account. Yet, the distribution of quantized DCT coefficients deviate from that of original DCT coefficients. This is particularly obvious when the quality factor of JPEG compressed images is small. To address this problem, we first use a set of training images to learn the compound effect of forward DCT, quantization and dequantization in cascade. Then, a new IDCT kernel is learned to reverse the effect of such a pipeline. Experiments are conducted to demonstrate that the advantage of the new method, which has a gain of 0.11-0.30dB over the standard JPEG over a wide range of quality factors.

## I. INTRODUCTION

Many image and video compression standards have been developed in the last thirty years. Examples include JPEG [1], JPEG2000 [2], and BPG [3] for image compression and MPEG-1 [4], MPEG-2 [5], MPEG-4 [6], H.264/AVC [7] and HEVC [8] for video compression. Yet, we see few machine learning techniques adopted by them. As machine learning becomes more popular in multimedia computing and content understanding, it is interesting to see how machine learning can be introduced to boost the performance of image/video coding performance. In this work, we investigate how machine learning can be used in the optimal design of the inverse discrete cosine transform (IDCT) targeting at quantization error compensation.

Block transforms are widely used in image and video coding standards for energy compaction in the spatial domain. Only a few leading DCT coefficients have larger magnitudes after the transformation. Furthermore, a large number of quantized coefficients become zeros after quantization. These two factors contribute to file size reduction greatly. The 8x8 block DCT [9] is used in JPEG. The integer cosine transform (ICT) is adopted by H.264/AVC for lower computational complexity. All forward and inverse kernels are fixed in these standards.

Research on IDCT has primarily focused on complexity reduction via new computational algorithms and efficient software/hardware implementation. For example, an adaptive algorithm was proposed in [10] to reduce the IDCT complexity. A zero-coefficient-aware butterfly IDCT algorithm was investigated in [11] for faster decoding. As to effective implementations, a fast multiplier implementation was studied in [12], where the modified Loeffler algorithm was implemented

on the FPGA to optimize the speed and the area. There is however little work on analyzing the difference of DCT coefficients before and after quantization. In image/video coding, DCT coefficients go through quantization and de-quantization before their inverse transform. When the coding bit rate is high, quantized-and-then-dequantized DCT coefficients are very close to the input DCT coefficients. Consequently, IDCT can reconstruct input image patches reasonably well.

However, when the coding bit rate is low, this condition does not hold any longer. The quantization effect is not negligible. The distribution of quantized DCT coefficients deviates from that of original DCT coefficients. The traditional IDCT kernel, which is derived from the forward DCT kernel, is not optimal. In this work, we attempt to find the optimal IDCT kernel. This new kernel is derived from the training set using machine learning approach. Simply speaking, it transforms quantized DCT coefficients back to spatial-domain pixel values, which is exactly what IDCT is supposed to do. Our solution can account for the quantization effect through the training of real world data so that the quantization error can be reduced in decoding. It can improve the evaluation score and visual quality of reconstructed images without any extra cost in decoding stage.

The rest of this paper is organized as follows. The impact of quantization on the IDCT is analyzed in Sec. II. The new IDCT method is proposed in Sec. III. Experiment results are presented in Sec. IV. Finally, concluding remarks and future research directions are given in Sec. V.

## II. IMPACT OF QUANTIZATION ON INVERSE DCT

The forward block DCT can be written as

$$\mathbf{X} = K\mathbf{x}, \quad (1)$$

where  $\mathbf{x} \in R^N$ ,  $N = n \times n$ , is an N-dimensional vector that represents an input image block of  $n \times n$  pixels,  $K \in R^{N \times N}$  denotes the DCT transform matrix, and  $\mathbf{X} \in R^N$  is the vector of transformed DCT coefficients. Rows of  $K$  are mutually orthogonal. Furthermore, they are normalized in principle. In the implementation of H.264/AVC and HEVC, rows of  $K$  may not be normalized to avoid floating point computation, which could vary from one machine to the other. Mathematically, we can still view  $K$  as a normalized kernel for simplicity. Then, the corresponding inverse DCT can be represented by

$$\mathbf{x}_q = K^{-1}\mathbf{X}_q = K^T\mathbf{X}_q, \quad (2)$$

where  $K^{-1} = K^T$  since  $K$  is an orthogonal transform and  $\mathbf{X}_q$  is the vector of quantized DCT coefficients. Mathematically, we have

$$\mathbf{X}_q = \text{DeQuan}(\text{Quan}(\mathbf{X})), \quad (3)$$

where  $\text{Quan}(\cdot)$  represents the quantization operation and  $\text{DeQuan}(\cdot)$  represents the de-quantization operation. If there is little information loss in the quantization process (i.e., nearly lossless compression), we have  $\mathbf{X}_q \approx \mathbf{X}$ . Consequently, the reconstructed image block  $\mathbf{x}_q$  will be close to the input image block,  $\mathbf{x}$ . Sometimes, a smaller compressed file size at the expense of lower quality is used. Then, the difference between  $\mathbf{X}_q$  and  $\mathbf{X}$  can be expressed as

$$\mathbf{e}_q = \mathbf{X} - \mathbf{X}_q. \quad (4)$$

In decoding, we have  $\mathbf{X}_q$  rather than  $\mathbf{X}$ . If we apply the traditional IDCT (i.e.,  $K^{-1} = K^T$ ) to  $\mathbf{X}_q$ , we can derive the image block error based on Eqs. (2), (2) and (4) as

$$\mathbf{e}_q = \mathbf{x} - K^{-1}\text{DeQuan}[\text{Quan}(K\mathbf{x})]. \quad (5)$$

To minimize  $\mathbf{e}_q$ , we demand that

$$K_q^{-1} \approx \text{DeQuan} \odot \text{Quan} \odot K \quad (6)$$

where  $\odot$  denotes an element-wise operation. Since it is difficult to find a mathematical model for the right-hand-side of Eq. (6), we adopt a machine learning approach to learn the relationship between quantized DCT coefficients,  $\mathbf{X}_q$ , and pixels of the original input block,  $\mathbf{x}$ , from a large number of training samples. Then, given  $\mathbf{X}_q$ , we can predict target  $\mathbf{x}$ .

### III. PROPOSED IDCT METHOD

We use image block samples of size  $8 \times 8$  to learn the optimal IDCT matrix. The training procedure is stated below.

- 1) Perform the forward DCT on each image block.
- 2) Quantize DCT coefficients with respect to quality factor  $QF$ .
- 3) Conduct linear regression between de-quantized DCT coefficients, which are the input, and image pixels of input blocks, which are the output, to determine optimal IDCT matrix  $\hat{K}$ .

Then, we will use  $\hat{K}$ , instead of  $K^{-1}$  in Eq. (5), for the IDCT task. Note that it is costly to train  $\hat{K}$  at every QF value.

For Step 2, it is important to emphasize that there is no need to train and store  $\hat{K}$  for every QF value, which is too costly. Instead, we can train and store several  $\hat{K}$  for a small set of selected quality factors. Then, according to the QF that is used to encode images, we can choose the  $\hat{K}$  with the closest QF to decode them. This point will be elaborated in Sec. IV.

For Step 3, we first reshape the 2D layout of image pixels and dequantized DCT coefficients (both of dimension  $8 \times 8$ ) into 1D vectors of dimension 64. Notation  $\mathbf{x}_i$  denotes the flattened pixel vector of the  $i$ th image block and

$$\mathbf{X}_{q,i} = \text{DeQuan}[\text{Quan}(K\mathbf{x}_i)] \quad (7)$$

denotes the flattened dequantized DCT coefficients of the  $i$ th image block. Next, we form data matrix  $P \in R^{64 \times N}$  of image

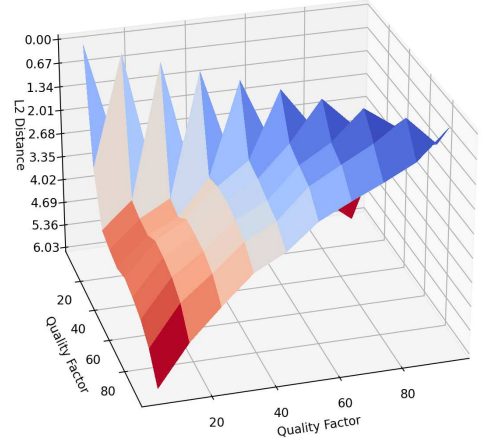


Fig. 1: The  $L_2$  norm of differences between kernels learned with different QFs.

pixels and data matrix  $D \in R^{64 \times N}$  of dequantized DCT coefficients. Columns of matrix  $P$  are formed by  $\mathbf{x}_i$  while columns of matrix  $D$  are formed by  $\mathbf{X}_{q,i}$ ,  $i = 1, \dots, N$ . Then, we can set up the regression problem by minimizing the following objective function

$$\xi(\hat{K}) = \sum_{i=1}^N \|\mathbf{e}_i\|^2, \quad (8)$$

where  $\|\cdot\|$  is the Euclidean norm and  $\mathbf{e}_i$  is the column vector of error matrix

$$E = P - \hat{K}D, \quad (9)$$

and where learned kernel,  $\hat{K}$ , is the regression matrix of dimension  $64 \times 64$ . Typically, the sample number,  $N$ , is significantly larger than  $64^2 = 4,096$ .

### IV. EXPERIMENTS

**Experimental Setup.** We perform experiments on three datasets with the libjpeg software [13] on a Unix machine. The three datasets are: Kodak [14], DIV2K [15], and Multiband Texture (MBT) [16]. The first two datasets contain generic images. They are used to test the power of the proposed IDCT method in typical images. The third dataset has specific content and it is desired to see whether our solution can be tailored to it for more performance gain. For each dataset, we split images into disjoint sets - one for training and the other for testing. There are 24, 785 and 112 total images in Kodak, DIV2K, and MBT datasets, and we choose 10, 100 and 20 from them as training images, respectively. The DCT remains the same as that in libjpeg. The IDCT kernel is learned at a certain QF based on discussion in Sec. III. Afterwards, the learned kernel is used to decode images compressed by libjpeg. Both RGB-PSNR and SSIM [17] metrics are used to evaluate the quality of decoded images.

**Impact of QF Mismatch.** It is impractical to train many kernels with different QF values. To see the QF mismatch effect on kernel learning, we show the  $L_2$  norm of differences

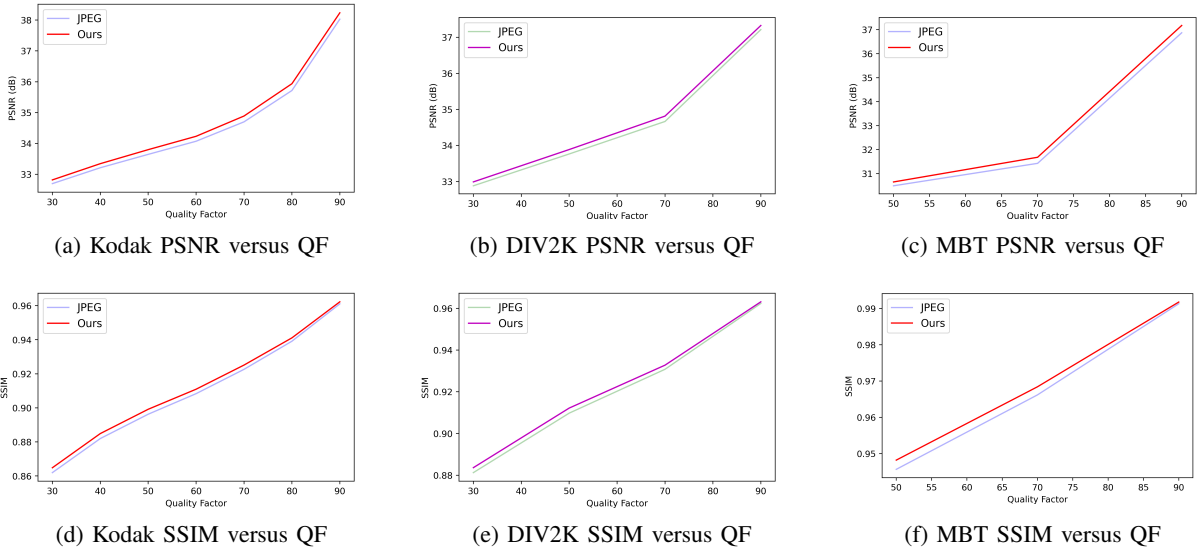


Fig. 2: Comparison of quality of decoded test images using the standard IDCT in JPEG and the proposed optimal IDCT for the Kodak, DIV2K and MBT datasets.

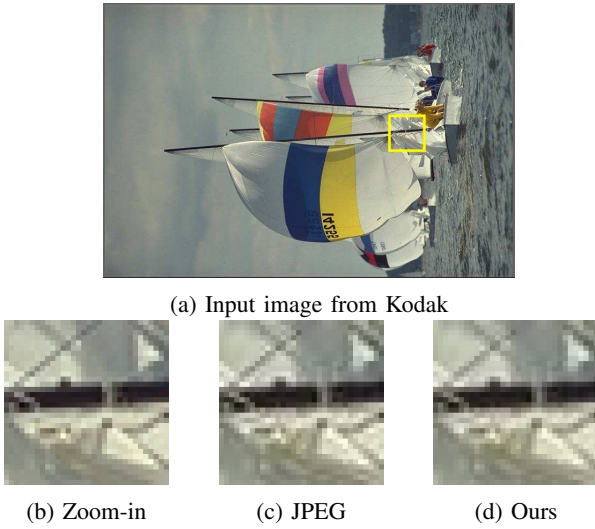


Fig. 3: Visualization of a zoom-in region of an input Kodak image, the decoded region by JPEG and the proposed method with QF=70.

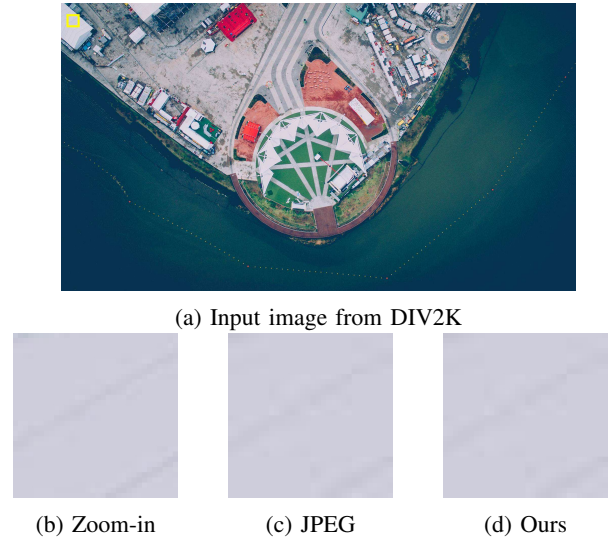


Fig. 4: Visualization of a zoom-in region from an input DIV2K image, the decoded region by JPEG and the proposed method with QF=70.

between learned kernels derived by different QFs in Fig. 1. We see from the figure that the kernel learned from a certain QF is close to those computed from its neighbouring QF values except for very small QF values (say, less than 20). When QF is very small, quantized DCT coefficients have a lot of zeros especially in high frequency region. This makes linear regression poor. The IDCT kernel derived from these quantized coefficients contains more zeros in each column which makes it different from others. We plot the PSNR value and the SSIM value of decoded test images using the standard IDCT in JPEG and the proposed optimal IDCT as a function of QF

in Fig. 2. We see a clear gain across all QFs and all datasets. Furthermore, we show the averaged PSNR and SSIM gains offered by the proposed IDCT designed with the fixed QF values over the standard DCT in Table I. The PSNR gain ranges from 0.11-0.30dB.

**Quality Comparison via Visual Inspection.** We show a zoom-in region of three representative images, each of which is selected from Kodak, DIV2K and MBT datasets using the standard IDCT and the proposed IDCT for visual inspection in Figs. 3, 4 and 5, respectively. The proposed IDCT method gives better edge, smooth and texture regions over the standard

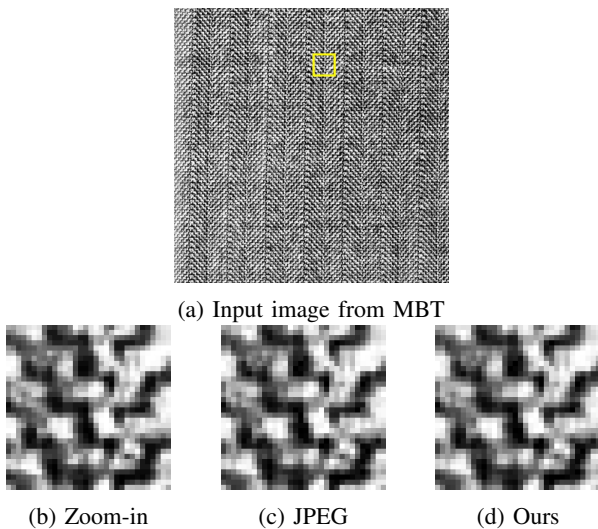


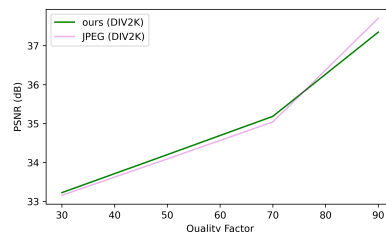
Fig. 5: Visualization of a zoom-in region of an input image from MBT, the decoded region by JPEG and the proposed method with QF=70.

		QF		
		50	70	90
Kodak	PSNR (dB)	+0.1930	+0.2189	+0.2057
	SSIM	+0.0029	+0.0025	+0.0012
DIV2K	PSNR (dB)	+0.1229	+0.1488	+0.1144
	SSIM	+0.0024	+0.0020	+0.0008
MBT	PSNR (dB)	+0.1603	+0.2537	+0.3038
	SSIM	+0.0025	+0.0022	+0.0005

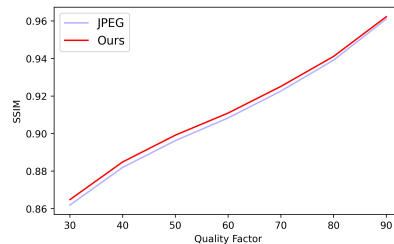
TABLE I: Evaluation results on test images in the Kodak, DIV2K, and MBT datasets, where training QFs are set to 50, 70 and 90 for each column.

IDCT in these three examples. Specifically, edge boundaries suffer less from the Gibbs phenomenon due to the learned kernel. Similarly, texture regions are better preserved and the smooth regions close to edge boundaries are smoother using the learned kernel. All familiar quantization artifacts decrease by a certain degree.

**Impact of Image Content.** Another phenomenon of interest is the relationship between image content and the performance of the proposed IDCT method. On one hand, we would like to argue that the learned IDCT kernel is generally applicable. It is not too sensitive to image content. To demonstrate this point, we use 10 images from the Kodak dataset to train the IDCT kernel with QF=70 and then apply it to all images in the DIV2K dataset. This kernel offers a PSNR gain of 0.24dB over the standard IDCT kernel. On the other hand, it is still advantageous if the training and testing image content matches well. As shown in Table I, MBT has a higher PSNR gain than Kodak and DIV2K. It is well known that texture images contain high-frequency components. When QF is smaller, these components are quantized to zero and it is



(a) PSNR versus QF



(b) SSIM versus QF

Fig. 6: Comparison of quality of decoded images using the standard IDCT and the proposed IDCT trained by the Kodak dataset yet tested on the DIV2K dataset.

difficult to learn a good kernel. Yet, when QF is larger, high-frequency components are retained and the learned kernel can compensate quantization errors better for a larger PSNR gain on the whole dataset.

## V. CONCLUSION AND FUTURE WORK

An IDCT kernel learning method that compensates the quantization effect was proposed in this work. The proposed method adopts a machine learning method to estimate the optimal IDCT kernel based on the quantized DCT coefficients and the desired output block of image pixels. Extensive experiments were conducted to demonstrate a clear advantage of this new approach. The learned kernel is not sensitive to the learning QF values neither to the image content. It offers a robust PSNR gain from 0.1 to 0.3 dB over the standard JPEG. Since it is used in the decoder, it does increase encoding time or the compressed file size. The learned kernel can be transmitted offline as an overhead file or simply implemented by the decoder alone.

It is interesting to consider region adaptive kernels. For example, we can roughly categorize regions into smooth, edge and textured regions. The distribution of DCT coefficients in these regions are quite different. Thus, we can use a clustering technique to group similar DCT coefficient distributions and conduct learning within a cluster. Furthermore, we may consider separable IDCT kernels since they can be implemented more effectively. Finally, it is desired to apply the same idea to video coding such as H.264/AVC and HEVC for further performance improvement.

## REFERENCES

- [1] G. K. Wallace, "The jpeg still picture compression standard," *IEEE transactions on consumer electronics*, vol. 38, no. 1, pp. xviii–xxxiv, 1992.
- [2] M. Rabbani, "Jpeg2000: Image compression fundamentals, standards and practice," *Journal of Electronic Imaging*, vol. 11, no. 2, p. 286, 2002.
- [3] *Better Portable Graphics*. [Online]. Available: <https://bellard.org/bpg/>
- [4] K. Brandenburg and G. Stoll, "Iso/mpeg-1 audio: A generic standard for coding of high-quality digital audio," *Journal of the Audio Engineering Society*, vol. 42, no. 10, pp. 780–792, 1994.
- [5] B. G. Haskell, A. Puri, and A. N. Netravali, *Digital video: an introduction to MPEG-2*. Springer Science & Business Media, 1996.
- [6] F. C. Pereira, F. M. B. Pereira, F. C. Pereira, F. Pereira, and T. Ebrahimi, *The MPEG-4 book*. Prentice Hall Professional, 2002.
- [7] T. Wiegand, G. J. Sullivan, G. Bjontegaard, and A. Luthra, "Overview of the h. 264/avc video coding standard," *IEEE Transactions on circuits and systems for video technology*, vol. 13, no. 7, pp. 560–576, 2003.
- [8] G. J. Sullivan, J.-R. Ohm, W.-J. Han, and T. Wiegand, "Overview of the high efficiency video coding (hevc) standard," *IEEE Transactions on circuits and systems for video technology*, vol. 22, no. 12, pp. 1649–1668, 2012.
- [9] N. Ahmed, T. Natarajan, and K. R. Rao, "Discrete cosine transform," *IEEE transactions on Computers*, vol. 100, no. 1, pp. 90–93, 1974.
- [10] I.-M. Pao and M.-T. Sun, "Modeling dct coefficients for fast video encoding," *IEEE Transactions on Circuits and Systems for Video Technology*, vol. 9, no. 4, pp. 608–616, 1999.
- [11] S.-h. Park, K. Choi, and E. S. Jang, "Zero coefficient-aware fast butterfly-based inverse discrete cosine transform algorithm," *IET Image Processing*, vol. 10, no. 2, pp. 89–100, 2016.
- [12] A. B. Atitallah, P. Kadionik, F. Ghozzi, P. Nouel, N. Masmoudi, and P. Marchegay, "Optimization and implementation on fpga of the dct/idct algorithm," in *2006 IEEE International Conference on Acoustics Speech and Signal Processing Proceedings*, vol. 3. IEEE, 2006, pp. III–III.
- [13] *libjpeg*. [Online]. Available: <http://libjpeg.sourceforge.net>
- [14] *Kodak images*. [Online]. Available: <http://r0k.us/graphics/kodak/>
- [15] E. Agustsson and R. Timofte, "Ntire 2017 challenge on single image super-resolution: Dataset and study," in *The IEEE Conference on Computer Vision and Pattern Recognition (CVPR) Workshops*, July 2017.
- [16] S. Abdelmounaime and H. Dong-Chen, "New brodatz-based image databases for grayscale color and multiband texture analysis," *ISRN Machine Vision*, vol. 2013, 2013.
- [17] Z. Wang, A. C. Bovik, H. R. Sheikh, and E. P. Simoncelli, "Image quality assessment: from error visibility to structural similarity," *IEEE transactions on image processing*, vol. 13, no. 4, pp. 600–612, 2004.